



QCD under Rotation

Effects of imaginary and real rotations on QCD matter

Gaoqing Cao

School of Physics and Astronomy
Sun Yat-sen University

GC, arXiv: 2310.03310.

图片来源: 视觉中国 www.vcg.com

2023.11.12@Fudan

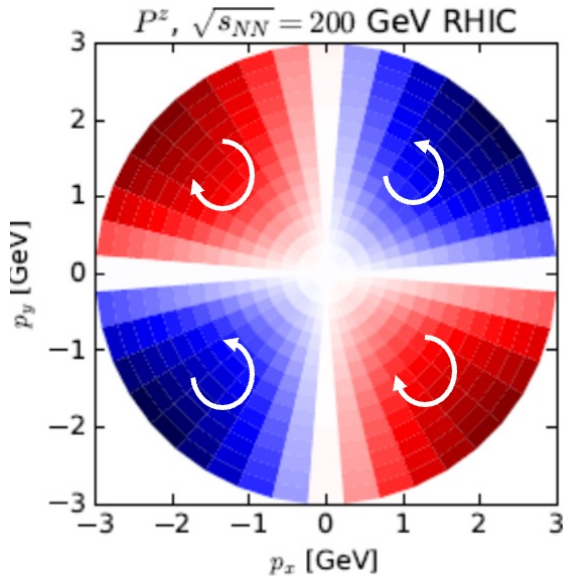
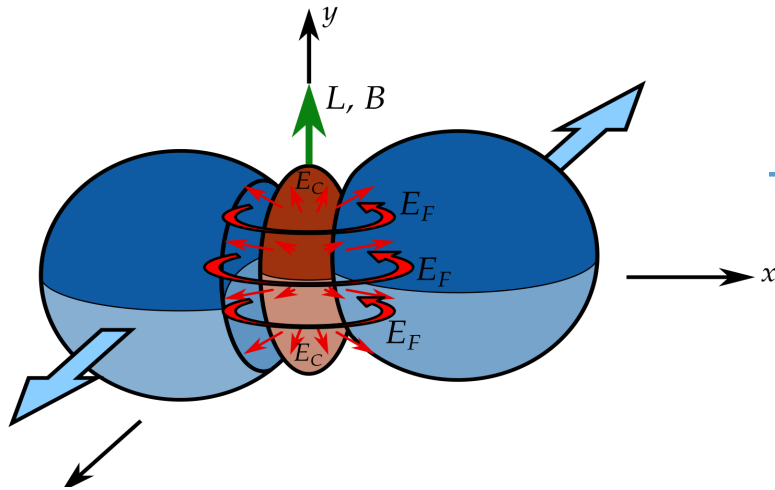


outline

- ◆ HIC and fast rotation
- ◆ Phase transitions in effective models
- ◆ Phase transitions in Lattice QCD
- ◆ Perturbative study
- ◆ Modified Polyakov loop potential
- ◆ Polyakov — Nambu—Jona-Lasinio model
- ◆ Summary and perspective



HIC and fast rotation



$\vec{\Omega} \parallel \vec{B}$ in heavy ion collisions

$$\Omega \sim 10^{22} s^{-1} \sim 6 \text{ MeV}$$

$$\Delta\epsilon \equiv \epsilon' - \epsilon = -S \cdot \omega$$

Ω plays a role of effective chemical potential

HIC is a good source of rotation

anomalous transport

magnetovorticity

K. Hattori & Y. Yin (PRL2016)

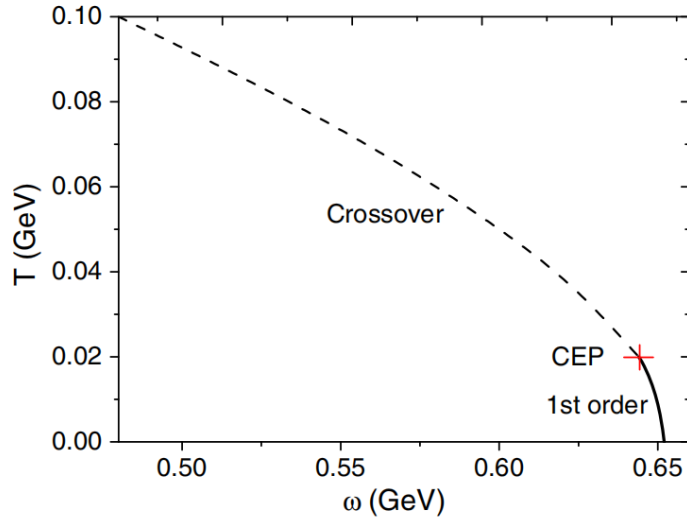
Chiral electric vortical effect

GC (PRD2021)



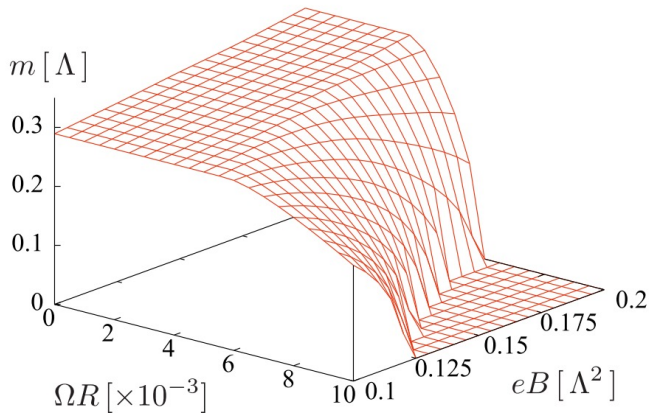
Phase transitions in effective models

NJL model



[Y. Jiang & J. Liao \(PRL2016\)](#)

1. Chiral symmetry restores with rotation
2. A critical end point

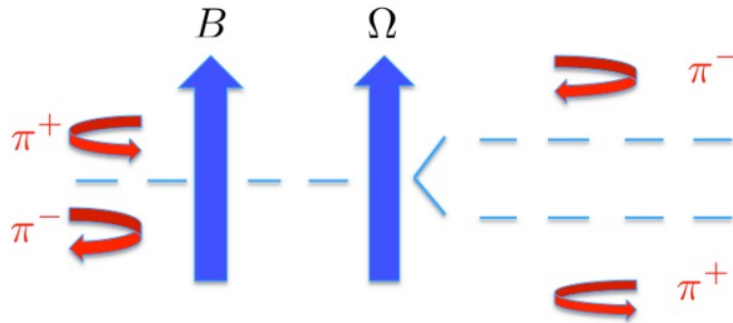


[H. Chen et.al. \(PRD2016\)](#)

- Chiral symmetry restores with magnetic field at large rotation
- de Haas-van Alphen effect



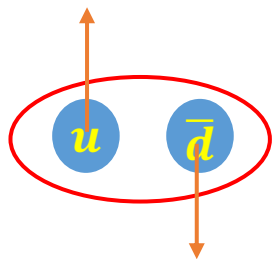
The case $\vec{\Omega} \parallel \vec{B}$



Y. Liu & I. Zahed (PRL2017)

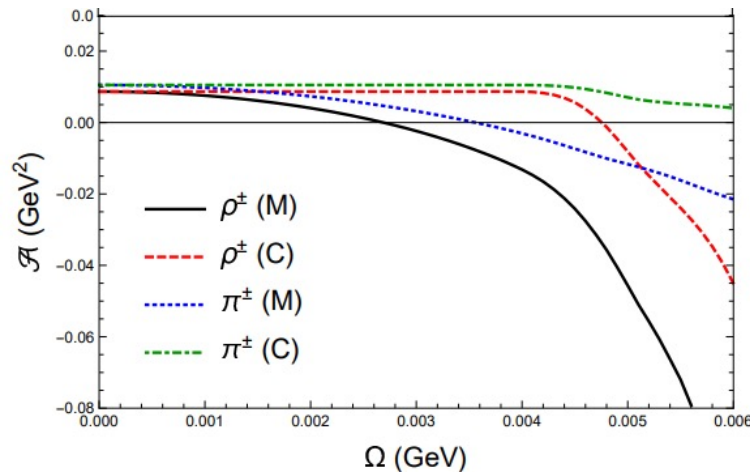
1. Energy splitting between π^- and π^+
2. Charge conservation: π^- and π^+ condensation in different region

Internal spin structure of π^+



Unstable with both Ω and B

GC & L. He (PRD2019, 2020)



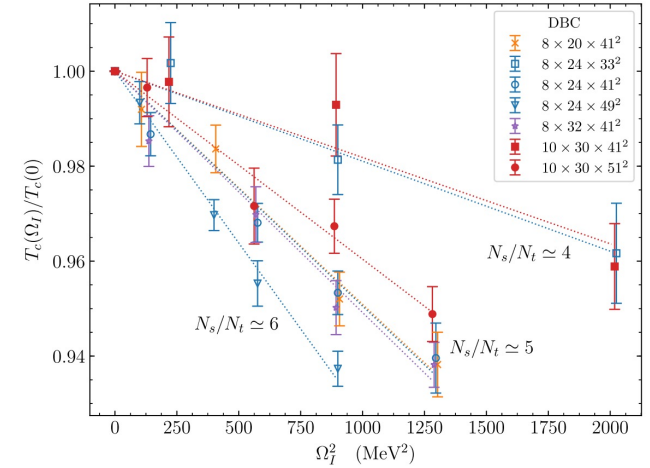
NJL model
 pion superfluid,
 rho superconductor
 ↓
 increasing isospin density



Phase transitions in Lattice QCD

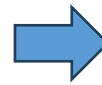
V. V. Braguta et.al. (PRD2021)

$$\begin{aligned}
 S_G = \frac{1}{2g^2} \int d^4x & [(1 - r^2\Omega^2)F_{xy}^a F_{xy}^a + (1 - y^2\Omega^2)F_{xz}^a F_{xz}^a \\
 & + (1 - x^2\Omega^2)F_{yz}^a F_{yz}^a + F_{xt}^a F_{xt}^a + F_{yt}^a F_{yt}^a \\
 & + F_{zt}^a F_{zt}^a - \underline{2iy\Omega}(F_{xy}^a F_{yt}^a + F_{xz}^a F_{zt}^a) \\
 & + \underline{2ix\Omega}(F_{yx}^a F_{xt}^a + F_{yz}^a F_{zt}^a) - 2xy\Omega^2 F_{xz}^a F_{zy}^a].
 \end{aligned}$$



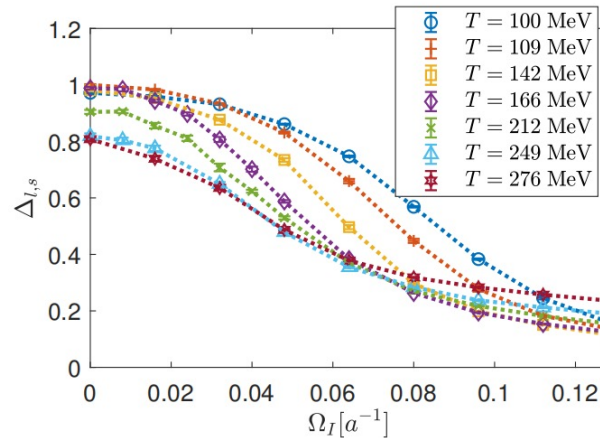
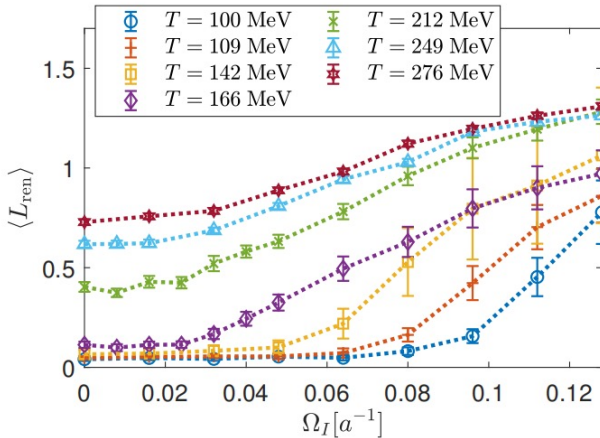
Imaginary rotation

$$\frac{T_c(\Omega_I)}{T_c(0)} = 1 - C_2 \Omega_I^2$$



Real rotation

$$\frac{T_c(\Omega)}{T_c(0)} = 1 + C_2 \Omega^2$$



J. Yang & X.G. Huang (2023)

Chiral symmetry restored by Ω_I



Perturbative study

Effective models

Holographic QCD: [D. Hou, M. Huang et.al. \(JHEP, PRD\).](#)

QM model: [H.L. Chen et.al. \(PRD2023\).](#)

NJL model: [Y. Jiang \(EPJC2022\).](#)

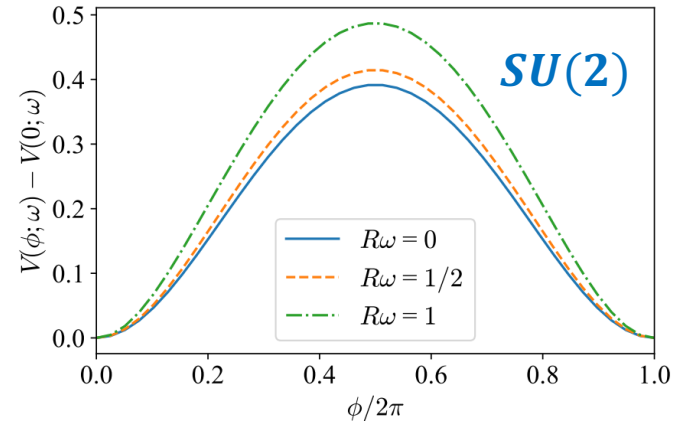
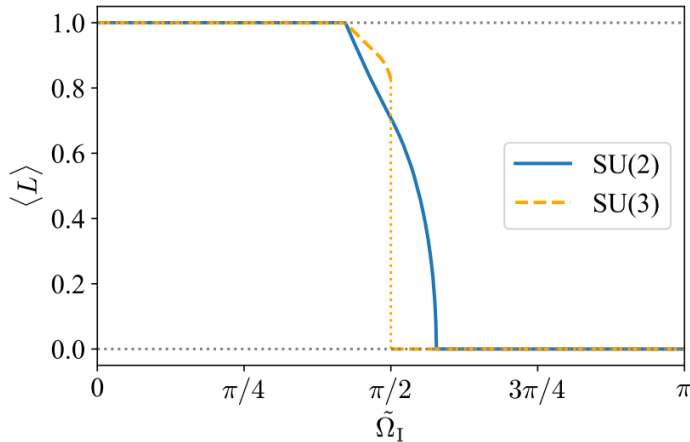
Bag model: [K. Mameda & K. Takizawa \(2023\).](#)

[K. Fukushima et.al. \(PRL2023\).](#)

nonphysical gluons
cancelled by ghosts

$$V = \frac{T}{4\pi^2} \sum_{\alpha} \sum_{m \in \mathbb{Z}} \int_0^{\infty} k_{\perp} dk_{\perp} \int_{-\infty}^{\infty} dk_z \left[\underline{J_{m-1}^2(k_{\perp} r)} + \underline{J_{m+1}^2(k_{\perp} r)} \right] \text{Re} \ln \left[1 - e^{-(|\vec{k}| - i\Omega_I m)/T + i\phi \cdot \alpha} \right].$$

Consistent with [M. N. Chernodub et.al. \(PRD2023\)](#)

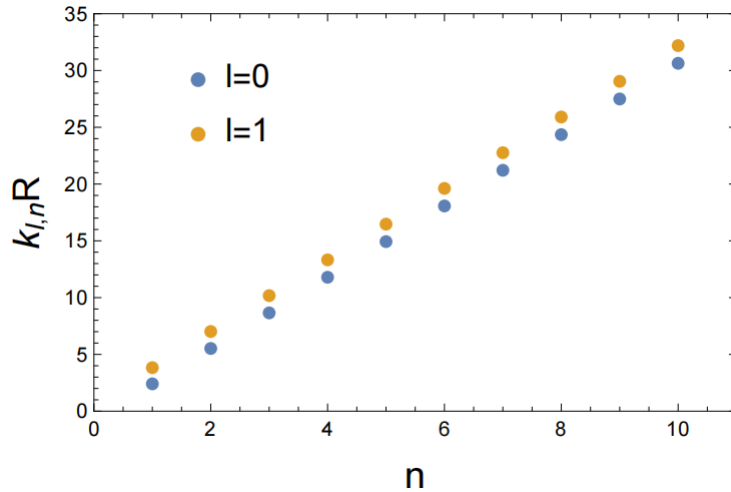




Modified Polyakov loop potential

Simple form: $V(\phi; \tilde{\Omega}_I)|_{\tilde{r}=0} = \frac{\pi^2 T^4}{3} \sum_{\alpha} \sum_{s=\pm 1} B_4 \left(\left(\frac{\phi \cdot \alpha + s \tilde{\Omega}_I}{2\pi} \right)_{\text{mod } 1} \right)$

Rotation can affect ghosts significantly in confined phase



$k_{l,n}$ the transversal eigenenergy

$$J_l(k_{l,n}R) = 0$$

$$k_{0,n} < k_{1,n} < k_{0,n+1} < k_{1,n+1}$$

Leading-order nontrivial approximation

$$\left[\begin{array}{l} \frac{V_1(L, L^*)}{T^4} = -\frac{a(\tilde{T})}{2} |L|^2 - \frac{1.75}{\tilde{T}^3} \ln H(L, L^*) \\ \frac{V_2(L, L^*)}{T^4} = -\frac{a(\tilde{T})}{2} |L|^2 - \frac{0.75}{6} (L^3 + L^{*3}) + \frac{7.5}{4} |L|^4 \end{array} \right] \rightarrow \left[\begin{array}{l} \bar{V}_1(q_{ij}, \Omega_I) = \frac{1}{2} \sum_{s=\pm} V_1(q_{ij} + s \Omega_I) \\ \bar{V}_2(q_{ij}, \Omega_I) = \frac{1}{2} \sum_{s=\pm} V_2(q_{ij} + s \Omega_I) \end{array} \right]$$

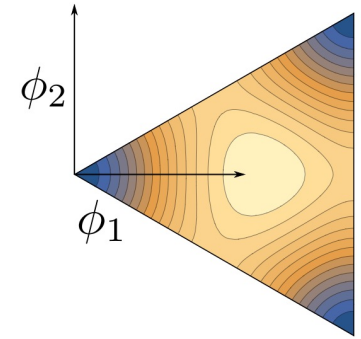


The results of V_1

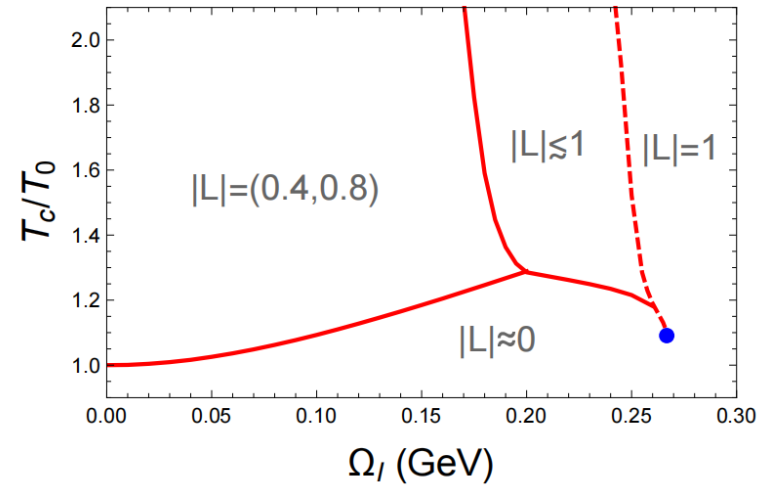
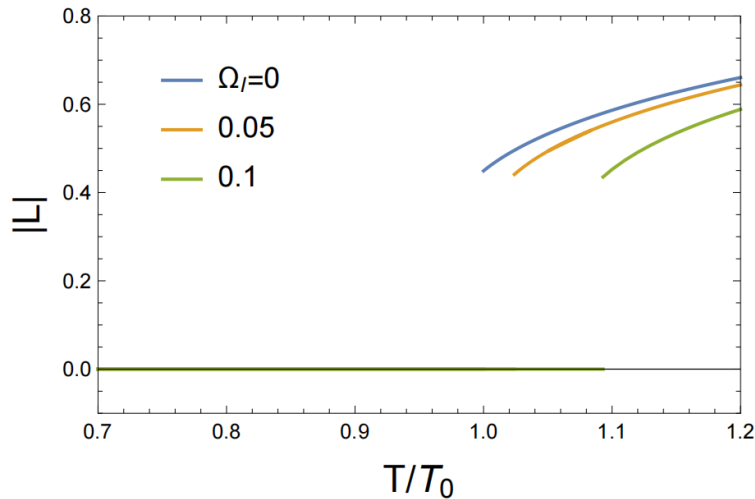
$$L(q_1, q_2, q_3) = \frac{1}{N_c} (e^{i q_1} + e^{i q_2} + e^{i q_3}) \quad q_{ij} = q_i - q_j$$

$$q_{31} = \phi_1, \quad q_{21} = \frac{\phi_1}{2} + \frac{\sqrt{3}}{2} \phi_2, \quad q_{32} = \frac{\phi_1}{2} - \frac{\sqrt{3}}{2} \phi_2$$

$$\phi_1 \in [0, 2\pi] \quad \phi_2 \in \left[-\frac{\phi_1}{\sqrt{3}}, \frac{\phi_1}{\sqrt{3}}\right]$$



Imaginary rotation



Several local minima

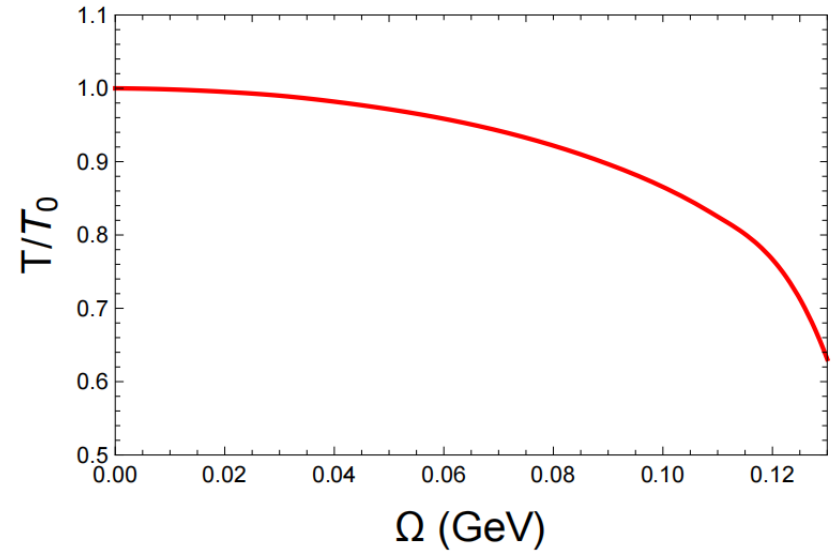
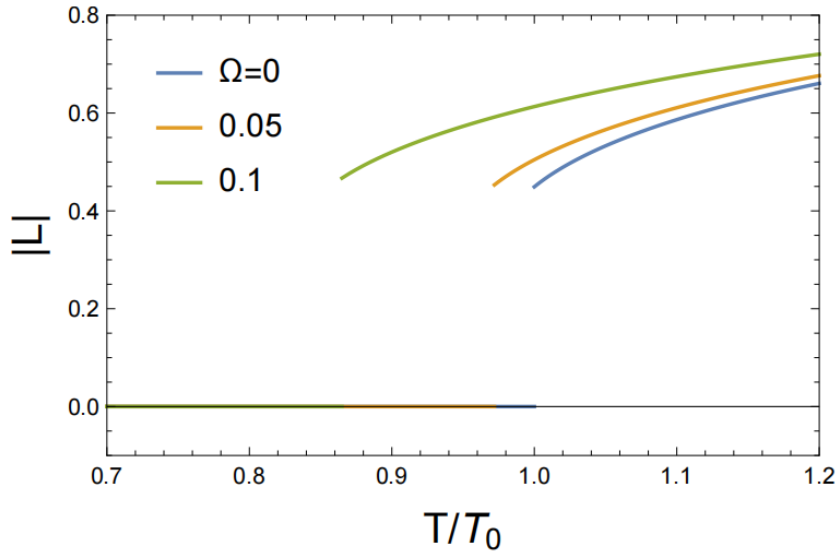


Several transition branches



The results of V_1

Real rotation



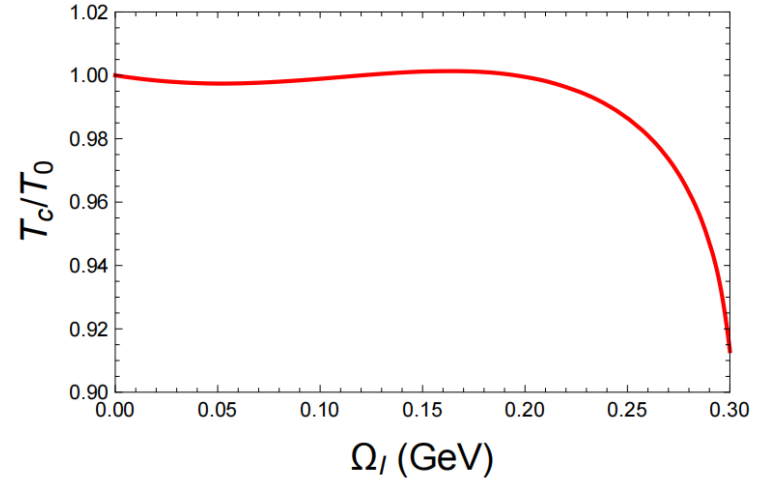
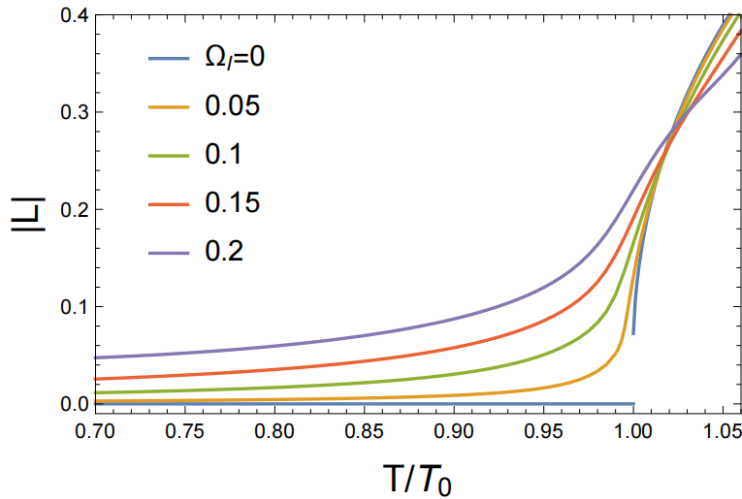
1. **First order transition** at any Ω

2. T_C **decreases** with Ω – **opposite to small Ω_I**

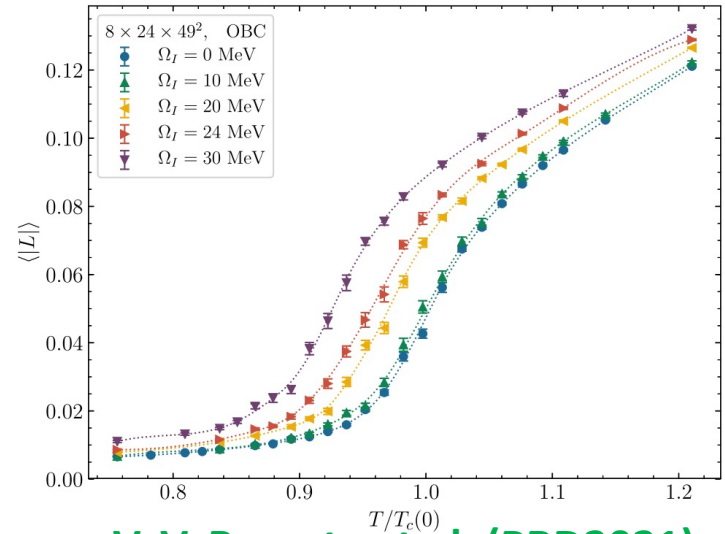


The results of V_2

Imaginary rotation



1. **Crossover transition** at larger Ω_I
2. T_c **decreases** with Ω_I basically
3. **Consistent** with **LQCD results**

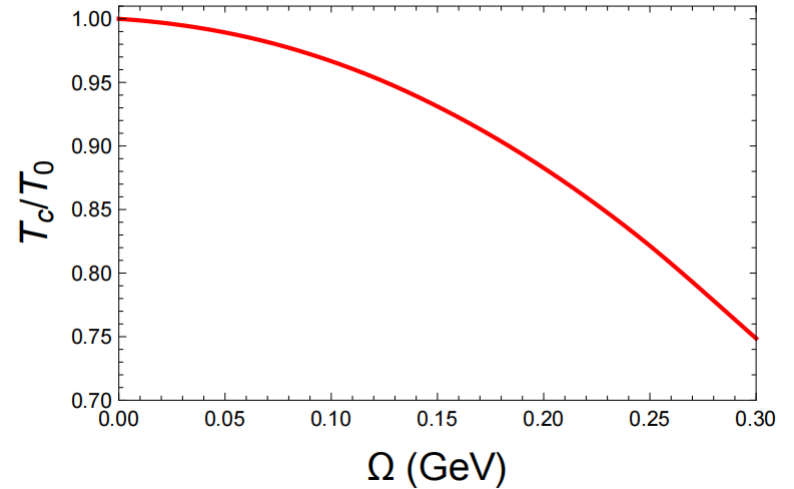
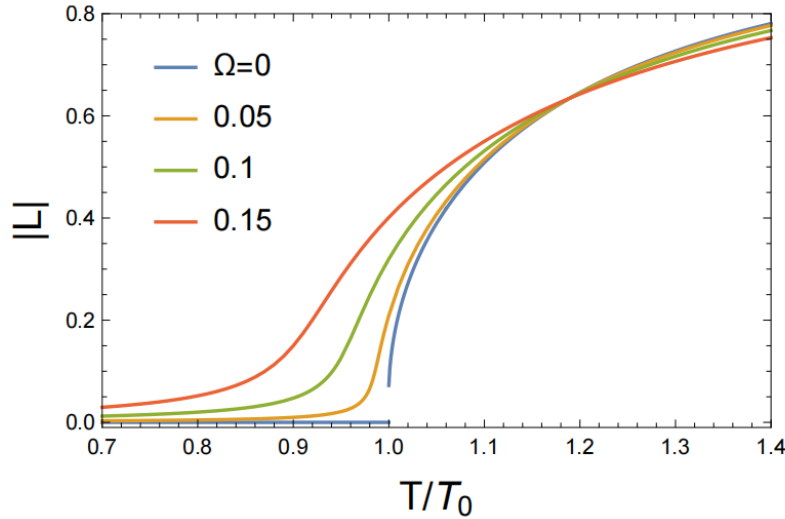


[V. V. Braguta et.al. \(PRD2021\)](#)



The results of V_2

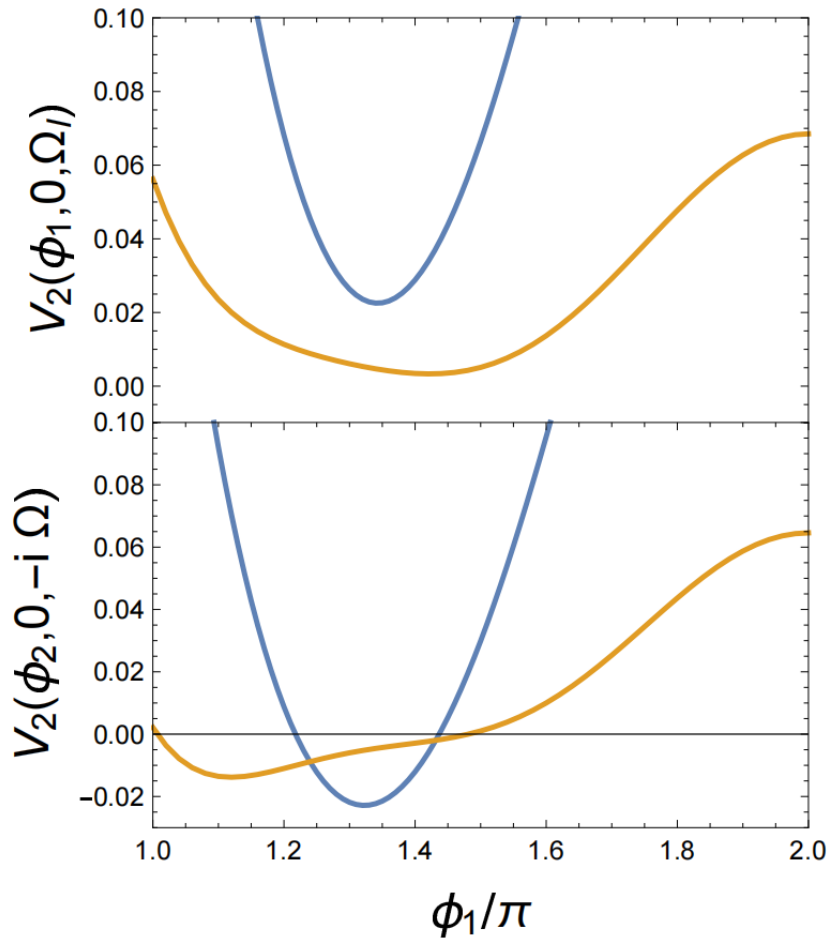
Real rotation



1. **Crossover transition** at larger Ω
2. T_c **decreases** with Ω
3. **Analytic continuation breaks down** for the phase diagram



Blue: $0.9 T_0$, Yellow: T_0



$$\phi_1 > \frac{4\pi}{3} \text{ for } \Omega_I$$



$$\text{Re } L < 0$$

$$\phi_2 < \frac{4\pi}{3} \text{ for } \Omega$$



$$\text{Re } L > 0$$



Polyakov — Nambu—Jona-Lasinio model

Three-flavor Lagrangian

$$\begin{aligned}
 \mathcal{L}_{\text{PNJL}} = & \bar{\psi} \left[i\cancel{\partial} - i\gamma^4 \left(\underline{ig\mathcal{A}_4} + i\Omega_I(\hat{L}_z + \hat{S}_z) \right) - m_0 \right] \psi \\
 & + G \sum_{a=0}^8 \left[(\bar{\psi}\lambda^a\psi)^2 + (\bar{\psi}i\gamma_5\lambda^a\psi)^2 \right] + \mathcal{L}_{\text{tH}} \\
 & - V_2(\phi_1, \phi_2, \Omega_I), \quad \boxed{g\mathcal{A}_4 = T \text{diag}(q_1, q_2, q_3)} \\
 \mathcal{L}_{\text{tH}} = & -\frac{K}{2} \sum_{t=\pm} \epsilon_{ijk}\epsilon_{imn} (\bar{\psi}^i\Gamma^t\psi^i)(\bar{\psi}^j\Gamma^t\psi^m)(\bar{\psi}^k\Gamma^t\psi^n)
 \end{aligned}$$

Thermodynamic potential with boundary condition

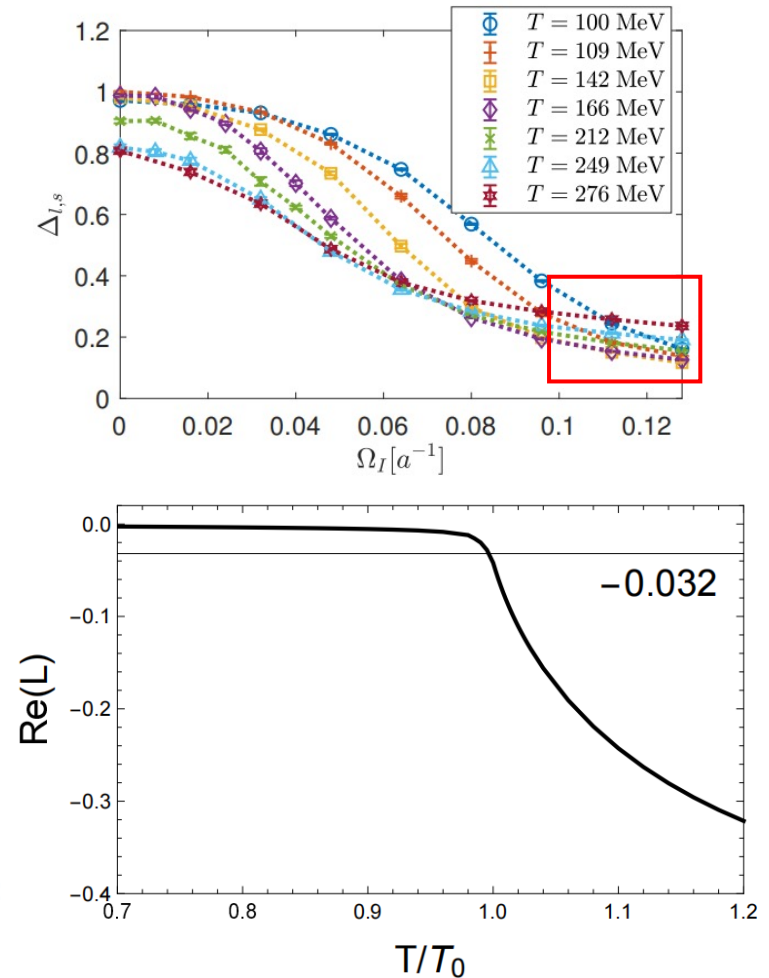
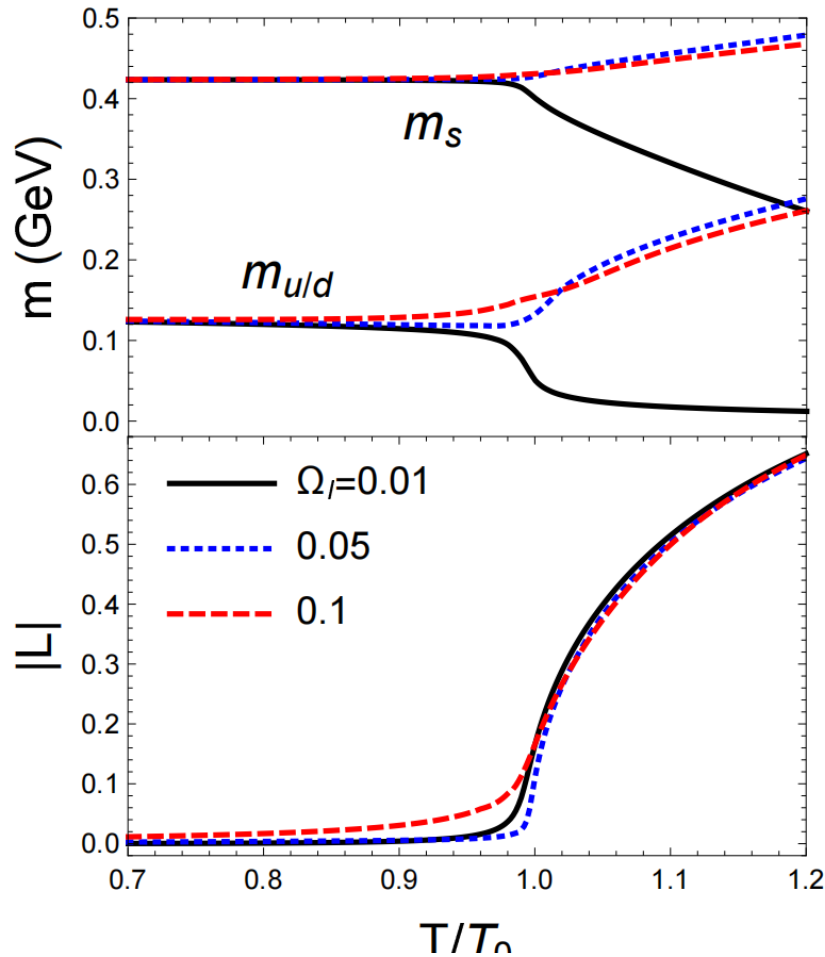
$$\begin{aligned}
 \Omega_{\text{bl}} = & - \sum_{f=u,d,s} \left[\sum_{l=0}^{\infty} \frac{1}{\pi^2 R^2} \sum_{n=1}^{\infty} \left\{ N_c \sum_{j=0}^3 (-1)^{j-1} C_3^j(\epsilon_{f0}^2 + j\Lambda^2) \ln(\epsilon_{f0}^2 + j\Lambda^2) \right. \right. \\
 & \left. \left. + 2T \sum_{t=\pm} \int_0^{\infty} dk_3 \left[\ln \left(1 + 3Le^{-\tilde{\epsilon}_f + i t(l+\frac{1}{2})\tilde{\Omega}_I} + 3L^* e^{-2\tilde{\epsilon}_f + 2i t(l+\frac{1}{2})\tilde{\Omega}_I} + e^{-3\tilde{\epsilon}_f + 3i t(l+\frac{1}{2})\tilde{\Omega}_I} \right) + c.c. \right] \right\} \right]
 \end{aligned}$$

$$\epsilon_f = \sqrt{k_{l,n}^2 + k_3^2 + m_f^2}$$

Real !



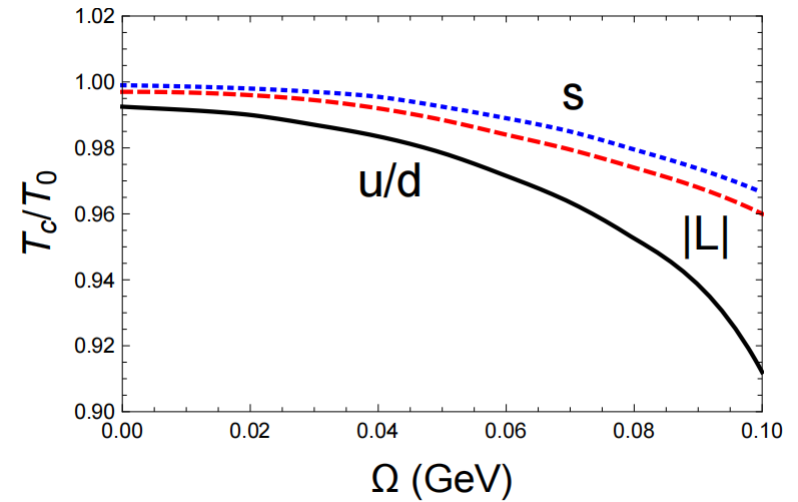
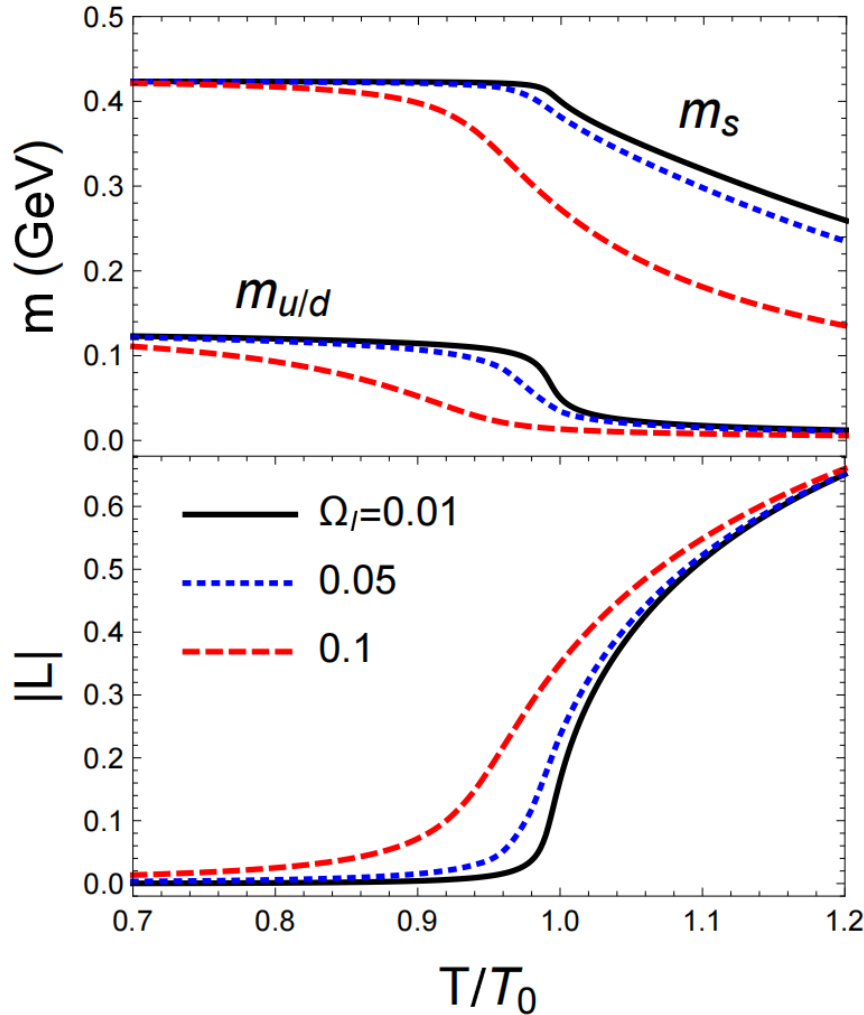
Results for imaginary rotation



$$Re \left[3Le^{-\tilde{\epsilon}_f + i \frac{t}{2} \tilde{\Omega}_I} + 3L^* e^{-2\tilde{\epsilon}_f + 2i \frac{t}{2} \tilde{\Omega}_I} + e^{-3\tilde{\epsilon}_f + 3i \frac{t}{2} \tilde{\Omega}_I} \right] < 0. \quad \Rightarrow \quad Re(L) < -0.032.$$



Results for real rotation



- 1. **crossover transition** for all Ω
- 2. T_c **decreases** with Ω

consistent with most **effective models**



Summary

- Polyakov loop potential **modified** according to **perturbative study**
- Munich's potential works very well
- Analytic continuation **breaks down** for the **phase diagram**
- The effects of **real rotation** are **consistent** with the expectations from **effective models**

Thank you very much !